Shoot-to-root mobile polypeptides involved in systemic regulation of nitrogen acquisition

Yuri Ohkubo[1], Mina Tanaka[1], Ryo Tabata, Mari Ogawa-Ohnishi and Yoshikatsu Matsubayashi*

Division of Biological Science, Graduate School of Science, Nagoya University

Chikusa, Nagoya 464-8602, Japan

TEL: +81-52-788-6176, FAX: +81-52-788-6178

[1]These authors contributed equally to this work

*Correspondence to: Y. Matsubayashi (matsu@bio.nagoya-u.ac.jp)

Main text

Plants uptake nitrogen (N) from the soil mainly in the form of nitrate. However, nitrate is often distributed heterogeneously in natural soil. Plants, therefore, have a systemic long-distance signaling mechanism by which N-starvation on one side of the root leads to a compensatory N uptake on the other N-rich side [1, 2]. This systemic N acquisition response is triggered by a root-to-shoot mobile peptide hormone, C-terminally Encoded Peptide (CEP), originating from the N-starved roots [3, 4], but the molecular nature of the descending shoot-to-root signal remains elusive. Here, we show that phloem-specific polypeptides that are induced in leaves upon perception of root-derived CEP act as descending long-distance mobile signals translocated to each root. These shoot-derived polypeptides, which we named CEP Downstream 1 (CEPD1) and CEPD2, upregulate the expression of the nitrate transporter gene *NRT2.1* in roots specifically when nitrate is present in the rhizosphere. *Arabidopsis* plants deficient in this pathway show impaired systemic N-acquisition response accompanied with N-deficiency symptoms. These fundamental mechanistic insights should provide a conceptual framework for understanding systemic nutrient acquisition responses in plants.

Plants have evolved sophisticated strategies allowing them to modulate the efficiency of root nitrate acquisition in response to fluctuating external nitrate availability. One striking example of such a nitrate acquisition system is when local N-starvation on one side of the root system leads to an upregulation of nitrate uptake in the other part of the root system [1, 2]. This compensatory nitrate acquisition response is called systemic N-demand signaling.

Recent findings revealed that systemic N-demand signaling is triggered by a small peptide hormone, C-terminally Encoded Peptide (CEP) [3, 4]. The *Arabidopsis* genome contains 15 CEP genes [5, 6], of which 7 are rapidly and highly upregulated in the portion of the root system directly experiencing N-starvation [3]. These 7 gene products are expressed in the stele of lateral roots and are loaded into the xylem vessels to act as root-derived ascending signals to the shoot. After translocation, CEP family peptides are perceived by a leucine-rich repeat receptor kinase (LRR-RK), CEP Receptor 1 (CEPR1), that is expressed in the vascular tissues of leaves [3]. Because loss of *CEPR1* leads to a loss of compensatory *NRT2.1* upregulation upon local N-starvation in roots, the CEP-CEPR system is a critical component of the systemic N-demand signaling. This conclusion is further supported by the observation

that the *Medicago truncatula CEPR1* ortholog *COMPACT ROOT ARCHITECTURE 2* (*CRA2*) also acts in the systemic pathway to regulate N acquisition [7].

Given that root-derived CEP family peptides are recognized by CEPR1 in leaf vascular tissues, we hypothesized that systemic N-demand signaling involves a descending shoot-to-root signal that is activated downstream of CEPR1. To address this possibility, we first investigated the expression pattern of CEPR1 receptor kinase in leaf vascular tissues. GUS reporter-aided histochemical analysis revealed that *CEPR1* promoter activity is restricted to the phloem cells in the vascular veins of both cotyledons and mature leaves (Fig. 1a-b). We also found that the *CEPR1* expression level is upregulated by N-starvation independently of CEP1, suggesting the possibility that the responsiveness of CEPR1 to root-derived CEP family peptides, which reflects the magnitude of local N-deficiency, is fine-tuned by the overall N-deficiency status of the plant (Supplementary Fig. 1).

The spatial expression pattern of CEPR1 receptor kinase raised the question of how root-derived CEP family peptides in xylem move to the phloem side within leaf vascular tissues. To answer this question, we chemically synthesized a fluorescent-labeled CEP1 that retains ≈40% of the biological activity of unmodified CEP1 at 1 μM (Alexa488-CEP1, Supplementary Fig. 2) and analyzed its molecular dynamics in leaves when applied to the roots. After 6 h of treatment, we detected marked accumulation of the Alexa488-CEP1 fluorescent signals in leaf veins most likely due to being concentrated by transpiration (Fig. 1c). Notably, a cross-section of leaf veins revealed that the fluorescent signal diffuses into the whole vascular bundle including phloem tissue (Fig. 1d). This evidence indicates that root-derived CEP is concentrated within the leaf vascular bundles and eventually reaches phloem cells.

To identify genes specifically induced downstream of CEPR1 activation, we isolated vascular tissues from cotyledons by cellulase-aided mechanical manipulation [8]. Successful isolation of the vasculature including CEPR1-expressing phloem cells was confirmed by the recovery of *proCEPR1:GFP* signals and enrichment of *CEPR1* transcripts in the collected tissues (Fig. 1e-g). We prepared total RNA from vascular tissues of wild type, CEP1-treated wild type, and *cepr1-1* mutant, and used a microarray analysis to identify genes specifically induced by CEP1. The combined results from the three samples identified 17 genes upregulated greater than 2-fold upon CEP1 treatment, as well as downregulated by 2-fold or more in the *cepr1-1* mutant (Supplementary Table 1). Among these, 14 genes were conserved

across seed plants, as do CEP family peptides [9], and 6 out of the 14 genes encode small proteins with no predicted secretion signal sequence.

We employed an overexpression screening strategy to identify a shoot-to-root secondary signal that is activated downstream of CEPR1, based on the assumption that overexpression of a possible secondary signal under the constitutive *35S* promoter induces *NRT2.1* expression in roots. We found that, among 6 primary candidate genes, *At1g06830* and *At2g47880* upregulated expression of *NRT2.1* by 4- to 7-fold when overexpressed, suggesting that they are strong candidates for secondary signals (Fig. 1h, Supplementary Fig. 3). At1g06830 and At2g47880 are currently assigned to the plant-specific class III glutaredoxin family [10], but, from a structural point of view, whether individual members of this family act in redox regulation remains controversial [11]. The class III glutaredoxin family comprises 21 members in *Arabidopsis* (Supplementary Fig. 4), among which ROXY1/2 are required for petal and anther development [12, 13] and AtGRXS3/4/5/8 negatively regulate root growth in response to cytokinin and nitrate [14]. The At1g06830/At2g47880 subfamily has not been functionally characterized to date. We excluded the remaining two members in this subfamily, *At2g30540* and *At3g62960*, from the detailed analysis, because the former shows no response to CEP1 and the latter displays no or negligible expression in leaf vasculature (Supplementary Table 2).

At1g06830 and *At2g47880* encode 98- and 102-amino-acid non-secreted polypeptides, respectively, with 85% sequence identity to each other (Fig. 1i). Both peptides were highly upregulated in shoots in a CEPR1-dependent manner when roots were treated with CEP1 (Fig. 1j). Similarly, *At1g06830* and *At2g47880* were highly induced upon N-starvation, although *At2g47880* was also partially regulated through a CEPR1-independent pathway (Supplementary Fig. 5). Elevated expression of *At1g06830* and *At2g47880* induced by N-starvation was returned to basal levels following N-resupply, indicating that *At1g06830* and *At2g47880* gene transcription is reversibly regulated by the N status of the roots (Supplementary Fig. 5). Induction of *At1g06830* and *At2g47880* was detectable after 2 h of CEP1 stimulation and reached almost plateau levels after 12 to 24 h (Fig. 1k). Dose-response analysis indicated that 10 nM CEP1 is able to upregulate *At1g06830* and 100 nM is able to upregulate *At2g47880*, values that agree with those required for *NRT2.1* induction (Fig. 1l) [3]. Importantly, overexpression of *At1g06830* and *At2g47880* specifically induced *NRT2.1* but not *NRT3.1* and *NRT1.1*, both of which have been shown to be upregulated by CEP1, albeit more slowly and weakly than *NRT2.1* (Supplementary Fig. 5) [3]. Thus, At1g06830 and

At2g47880 selectively direct *NRT2.1* among divergent downstream signaling pathways of CEPR1. The other well-characterized N-regulated genes, such as the gene encoding ammonium transporter AMT1.1, nitrate reductase NIA1, nitrite reductase NIR1, and nodule inception-like protein NLP7 were also non-responsive to At1g06830 and At2g47880 (Supplementary Fig. 5). Collectively, these results indicate that At1g06830 and At2g47880 act downstream of the CEP-CEPR ligand-receptor system to regulate *NRT2.1*, a central target of systemic N-demand signaling, and we named these two polypeptides CEP Downstream 1 (CEPD1) and CEPD2, respectively.

To further define the function of CEPD1 and CEPD2, we isolated mutants that carry T-DNA insertions in *CEPD1* and *CEPD2*, which we designated *cepd1-1* and *cepd2-1* (Fig. 2a). The insertion sites and the absence of full-length transcripts for these genes were confirmed by genomic PCR and RT-PCR (Fig. 2a, Supplementary Fig. 6). We observed that the *cepd1-1 cepd2-1* double mutant displays a CEP1-insensitive phenotype in terms of *NRT2.1* induction in roots (Fig. 2b). This phenotype was complemented by expressing a GFP-CEPD1 fusion protein under the control of its native promoter (Supplementary Fig. 6). The *cepd1-1* single mutant also exhibited less sensitivity to CEP1, suggesting a major role of CEPD1 and a minor but redundant role of CEPD2 in the relevant signaling pathways. The *cepd1-1 cepd2-1* double mutant plants produced longer lateral roots with slightly pale green leaves that are reminiscent of the *cepr1-1* receptor mutant (Fig. 2c, Supplementary Fig. 6) [3].

We used a split-root culture system, in which the root system of a plant is separated into two parts exposed to different N-availability conditions, to investigate whether CEPD1 and CEPD2 indeed mediate systemic N-demand signaling (Fig. 2d). We transferred one side of the split-root system to a medium devoid of N while the other side was kept in medium containing 10 mM nitrate. In wild-type plants, we observed upregulation of *NRT2.1* in the roots exposed to the N-rich medium after 24 h (Fig. 2e). In contrast, no such systemic upregulation of *NRT2.1* was detected in the roots of the *cepd1-1 cepd2-1* mutant. These results indicate that CEPD1 and CEPD2 polypeptides are critical components for systemic N-demand signaling.

Histochemical analyses of the transgenic *Arabidopsis* plants indicated that both *CEPD1* and *CEPD2* promoter activities are restricted to the phloem cells in the vascular veins of both cotyledons and mature leaves in shoots (Fig. 3a-d). Analysis by qRT-PCR further confirmed the shoot-specific localization of *CEPD1* and *CEPD2* transcripts, with no or only negligible levels of transcripts being detected in the roots, even after CEP1 treatment

(Supplementary Fig. 7). Notably, in contrast to their gene expression patterns, we observed considerable GFP-CEPD1 signals in the root vascular region of *cepd1-1 cepd2-1* plants complemented by *GFP-CEPD1* under the control of a native promoter (Fig. 3e). Accumulation of these GFP-CEPD1 signals in roots was enhanced by treatment with CEP1 (Fig. 3e). GFP-CEPD1 signals were also highly enhanced upon N-starvation, and returned to basal levels following N-resupply (Supplementary Fig. 7). An analysis of cross-sections of the primary roots showed that GFP-CEPD1 fluorescence was predominantly found in phloem cells but was also detected in the endodermis cell layer (Fig. 3f-g). On the subcellular level, GFP-CEPD1 appears to localize to both the nucleus and cytoplasm (Fig. 3h). These results strongly suggest that CEPD polypeptides function as shoot-to-root mobile signals acting downstream of CEPR1.

To unambiguously confirm that GFP-CEPD1 detected in roots is translocated from the shoot, we performed reciprocal grafting between *GFP-CEPD1*-complemented *cepd1-1 cepd2-1* seedlings and parental *cepd1-1 cepd2-1* seedlings. We observed a considerable accumulation of GFP-CEPD1 signal in roots accompanied with upregulation of *NRT2.1* expression when *GFP-CEPD1* scions were grafted onto *cepd1-1 cepd2-1* rootstocks by hypocotyl-to-hypocotyl grafting (Fig. 3i, Supplementary Fig. 7). No such GFP signals were, in contrast, detected in roots when *cepd1-1 cepd2-1* scions were grafted onto *GFP-CEPD1* rootstocks, excluding the possibility of *GFP-CEPD1* misexpression in roots. All these results indicate that CEPD polypeptides are graft-transmissible phloem-mobile signals from shoots to roots.

Finally, we addressed the question of how CEPD polypeptides induce *NRT2.1* expression, specifically in the side of the root system exposed to the N-rich medium under the heterogeneous N conditions. There are two possibilities to explain this response. One is that shoot-derived CEPD polypeptides are selectively translocated to the root system of the N-rich side in a direction-specific manner. The other possibility is that CEPDs distribute into both side of the root system but activate *NRT2.1* expression only in the roots where nitrate is available. To determine which possibility is correct, we first compared the levels of GFP-CEPD1 accumulation in each side of the root system under split-root conditions. There was, however, no apparent difference in the abundance of GFP-CEPD1 in the roots even when one side of the root system was subjected to N-starvation, thus eliminating the first possibility (Fig. 4a).

To test the second possibility, we analyzed the expression levels of *NRT2.1* in each side of the root system of *CEPD1*-overexpressing plants exposed to the heterogeneous N conditions. Remarkably, we found that *NRT2.1* expression was specifically induced in the roots exposed to the N-rich medium but not in the N-starved roots of the split-root system (Fig. 4b). *CEPD1* transcripts themselves were present at comparable levels between N-rich and N-starved roots (Supplementary Fig. 7). Similar results were observed for *CEPD2*-overexpressing plants exposed to the heterogeneous N conditions (Fig. 4c, Supplementary Fig. 7). We also confirmed that, when both sides of the roots of *CEPD1*-overexpressing plants were incubated in N-rich conditions, *NRT2.1* expression was equally induced in both roots (Fig. 4b-c). Collectively, our findings demonstrate that shoot-born CEPD polypeptides themselves translocate into each root system at the same rate, but they can activate *NRT2.1* expression specifically in the roots where nitrate is available.

The overall picture of the molecular mechanisms of systemic N-demand signaling that emerged from our analyses is as follows: (I) CEP family peptides upregulated on one side of the roots by local N-starvation act as xylem-mobile ascending N-demand signals to the shoot. (II) CEP accumulates in leaf xylem and diffuses into phloem tissues probably by the transpiration stream. (III) Recognition of CEP by CEPR on the surface of phloem cells leads to the production of CEPD polypeptides acting as phloem-mobile descending signals directed to each root. *CEPR* expression is enhanced by N-starvation, thus possibly facilitating the coordination of CEPD signaling with the overall N-deficiency status of the plant. (IV) Shoot-derived CEPD polypeptides upregulate *NRT2.1* expression in the roots specifically when nitrate is present in the rhizosphere, thereby compensating for the local N-deficiency at the whole-plant level. Thus, individual roots integrate shoot-derived N-demand signals with the information regarding the local nitrate availability in soil, and make a decision whether to upregulate *NRT2.1* or not. This nitrate-dependent *NRT2.1* induction by CEPD polypeptides may reflect the intrinsic nature of the *NRT2.1* gene, which exhibits nitrate-inducible expression [15]. These fundamental mechanistic insights should provide a conceptual framework for understanding the systemic starvation responses not only for nitrogen but also for the other essential nutrients such as phosphate and iron whose uptake is systemically regulated [16, 17].

Our results also suggest the possibility that plants make use of the transpiration system in leaves for the enrichment of root-derived weak, diluted signaling molecules to a level sufficient for receptor activation. Indeed, concentrations of root-to-shoot mobile

peptides in xylem sap were estimated to be at subnanomolar levels that are generally insufficient to trigger function [3, 18]. This may be one of the reasons why plants utilize the root-to-shoot-to-root pathway for root-to-root communication. Additionally, receptors exist in the phloem tissue which locates on the abaxial (lower) side relative to the xylem in leaves. Because transpiration rates are usually higher on the stomata-rich abaxial surface than on the adaxial (upper) side [19], this xylem/phloem positioning in leaves may be physiologically relevant in that transpiration flow directed toward the abaxial surface facilitates diffusion of the xylem-mediated signals into the phloem side. The abaxial side of the leaves is composed of a spongy parenchyma layer with large air spaces between cells through which water evaporates from the leaves, thereby likely allowing the root-derived signals to be concentrated on the surface of the leaf veins. Thus, plants, despite having a relatively simple body organization, have evolved sophisticated long-distance signaling mechanisms to respond to environmental fluctuations by taking full-advantage of the available tissue systems.

Methods

Plant materials and growth conditions. *Arabidopsis thaliana* ecotype Nössen was used as wild type. The *cepr1-1* and *cepd2-1* mutants (Nössen background) were obtained from the RIKEN *Arabidopsis* transposon mutant collection (RATM11-2459 and RATM13-0053, respectively) [20]. The *cepd1-1* mutant (Columbia background) is a Salk T-DNA insertion line [21] and was obtained from the Arabidopsis Biological Resource Center (SALKseq_086598). This *cepd1-1* mutant was backcrossed twice to wild-type Nössen before characterization. Surface-sterilized seeds were sown in plates on solid medium containing modified Murashige-Skoog (MS) basal salts and 0.5% sucrose. Modified MS medium for N-rich conditions (N-rich medium) contains 10 mM NH_4Cl and 10 mM KNO_3 as the N and K sources, respectively, and half-strength concentrations of the other elements, and was adjusted to pH 5.8 with KOH. For N-starvation medium, NH_4Cl and KNO_3 were omitted and 10 mM KCl was added. For normal culture, 8 seeds were sown on medium solidified using 0.7% agar in Petri dishes. For vertical culture, 12 seeds were sown on medium solidified using 1.5% agar in 13 × 10 cm plastic plates. For peptide treatment, CEP1 peptide was added to the medium at 1 μM, unless otherwise stated. Plants were grown at 22°C with continuous light at an intensity of 50 $\mu mol \cdot m^{-2} \cdot s^{-1}$.

Synthesis of Alexa488-CEP1. The Fmoc-protected CEP1 analog Fmoc-[Lys^3]CEP1 was synthesized by Fmoc chemistry using a peptide synthesizer (Model 431A, Applied Biosystems). Alexa Fluor 488 succinimidyl ester (0.5 mg, Thermo Fisher), Fmoc-[Lys^3]CEP1 (3.0 mg), and $NaHCO_3$ (1.0 mg) were dissolved in 200 ml of 50% acetonitrile and stirred for 2 h in the dark at room temperature. Crude peptide was purified by reverse-phase HPLC and lyophilized to yield analytically pure Fmoc-[(Alexa488)Lys^3]CEP1. To this purified peptide was added 200 ml of 20% piperidine in acetonitrile, followed by incubation for 1 h in the dark at room temperature. This deprotected peptide was further purified by reverse-phase HPLC and lyophilized to obtain analytically pure [(Alexa488)Lys^3]CEP1 (Alexa488-CEP1).

Isolation of the vascular tissues from cotyledons. For vascular tissue isolation from cotyledons, ≈100 seeds were sown on N-rich medium solidified using 1.0% agar in 13 × 10 cm plastic plates. Cotyledons of 8-day-old seedlings were harvested and processed according

to the protocol of Endo *et al* [8]. In brief, ≈20 cotyledons were immersed in 1 ml of the enzyme solution (0.75% Cellulase Onozuka R-10 (Yakult), 0.25% Macerozyme R-10 (Yakult), 0.4 M mannitol, 5 mM MES-KOH (pH 5.6), 8 mM $CaCl_2$) in 1.5-ml tube and sonicated 3-5 times for 5 sec each with a Bioruptor UCD-250 (Cosmo Bio, Japan). Macerated cotyledons were spread on a Petri dish and vascular tissues were manually collected under a stereomicroscope. Isolated tissues were directly dropped into 450 μl RLT buffer provided in an RNeasy Plant Mini Kit (QIAGEN) in 1.5-ml tubes and the RNA was isolated. Total RNA for microarray analysis was isolated from the vascular tissues derived from ≈200 cotyledons.

Microarray analysis and qRT-PCR. Total RNA isolated from the vascular tissues derived from ≈200 cotyledons of wild type, wild type grown in the presence of 1 μM CEP1 and *cepr1-1* mutant were subjected to microarray analysis. Labeled complementary RNA was hybridized with an Affymetrix Genechip Arabidopsis Gene 1.0 ST array according to the manufacturer's protocol. The statistical significance in changes in transcript abundance was evaluated by Z-score, where absolute value above 2 was considered as significant. Real-time qRT-PCR was conducted as described previously [3].

Overexpression screening. We obtained the ORFs of each gene by reverse transcription-PCR (RT-PCR) with cDNA from the cotyledons, and cloned them downstream of the CaMV 35S promoter in *Bam*HI/*Sac*I-digested pBI121 vector using an In-Fusion HD Cloning Kit (Clontech). Transgenic *Arabidopsis* plants were generated by the standard floral dip method.

Promoter analysis. For β-glucuronidase (GUS) reporter-aided analysis of the promoter activities of *CEPR1*, *CEPD1* and *CEPD2*, we amplified the 2.0-kb upstream sequences of the predicted ATG start codons of each gene by genomic PCR, and cloned them into a promoter-less pBI101 vector upstream of the GUS reporter gene using the In-Fusion cloning system (Clontech). GUS activity was visualized using X-Gluc as substrate using a conventional protocol. For GFP reporter-aided analysis of the *CEPR1* promoter activity, the 2.0-kb upstream sequence of *CEPR1* and the GFP coding sequence were cloned into the *Bam*HI/*Sac*I-digested binary vector pBI121 in this order by three-component ligation.

Complementation analysis. For complementation analysis, 2.0-kb upstream sequences of the predicted ATG start codon of *CEPD1*, GFP coding region and *CEPD1* ORF were ligated in-frame in this order into the *Hin*dIII/*Bam*HI-digested binary vector pCAMBIA1300-BASTA by four-component ligation using the In-Fusion cloning system. The *GFP-CEPD1* constructs were introduced into the *cepd1-1 cepd2-1* double mutant by *Agrobacterium*-mediated transformation.

Split-root experiments. Modified MS agar medium for split culture (split N-rich medium) contains 10 mM KNO_3 as N and K source, and half-strength concentrations of the other elements, 0.5% sucrose and 1.5% agar. To generate split roots, the primary roots of vertically grown 7-day-old seedlings were cut below the first two lateral roots, and the roots were allowed to grow for an additional 4 days. Then, each plant with two main roots was transferred onto a 10 cm petri dish with two compartments (Kord-Valmark #2903, USA) and cultured vertically for an additional 5 days. For split N-starvation experiments, plants displaying balanced roots on both sides were transferred onto a 10 cm petri dish with two compartments containing a split N-rich medium on one side and a N-starvation medium on the other side.

Grafting experiments. *Arabidopsis* seedlings were vertically grown for 8 days on N-rich medium before grafting. Grafting was aseptically performed by cutting the rootstock donor perpendicular to the hypocotyl using a surgical blade, then inserting the rootstock into a short length (≈2 mm) of sterile 0.4 mm diameter silicon tubing basically as described previously [22]. The scion was excised in a similar manner and inserted into the other end of the tubing until it touched the rootstock. Plants were grown for another 7 days and analyzed.

Imaging and microscopy. For leaf imaging, the Alexa488-CEP1 localization or CEPR1:GFP expression patterns were recorded with a stereomicroscope (Olympus SZX16). For leaf sectioning, leaves were fixed in FAA solution (3.7% formaldehyde, 5% acetic acid, and 50% ethanol), dehydrated through a graded ethanol series, and embedded in Technovit 7100 resin (Heraeus Kulzer, Germany) following the manufacturer's protocol. Sections were cut at 5 μm-thick using a rotary microtome (Leica RM2235), counter-stained with 0.05% Nile red, mounted with Entellan (Merck) and observed under a standard light microscope

(Olympus BX60). For root imaging, cell outlines were stained with 50 μg/ml propidium iodide for 2 min and observed under a confocal laser-scanning microscope (Olympus FV300) with helium-neon laser excitation at 543 nm. GFP images were collected with argon laser excitation at 488 nm. For vibratome sectioning of roots, primary roots were embedded in 6% agarose and sectioned at 250 μm-thick with a vibratome (Leica VT1200S).

References

1. Gansel, X., Munos, S., Tillard, P. & Gojon, A. Differential regulation of the NO_3^- and NH_4^+ transporter genes *AtNrt2.1* and *AtAmt1.1* in *Arabidopsis*: relation with long-distance and local controls by N status of the plant. *Plant J* **26**, 143-155 (2001).
2. Ruffel, S. *et al.* Nitrogen economics of root foraging: transitive closure of the nitrate-cytokinin relay and distinct systemic signaling for N supply vs. demand. *Proc Natl Acad Sci U S A* **108**, 18524-18529 (2011).
3. Tabata, R. *et al.* Perception of root-derived peptides by shoot LRR-RKs mediates systemic N-demand signaling. *Science* **346**, 343-346 (2014).
4. Ohyama, K., Ogawa, M. & Matsubayashi, Y. Identification of a biologically active, small, secreted peptide in *Arabidopsis* by *in silico* gene screening, followed by LC-MS-based structure analysis. *Plant J* **55**, 152-160 (2008).
5. Delay, C., Imin, N. & Djordjevic, M.A. *CEP* genes regulate root and shoot development in response to environmental cues and are specific to seed plants. *J Exp Bot* **64**, 5383-5394 (2013).
6. Roberts, I. *et al.* The CEP family in land plants: evolutionary analyses, expression studies, and role in *Arabidopsis* shoot development. *J Exp Bot* **64**, 5371-5381 (2013).
7. Huault, E. *et al.* Local and systemic regulation of plant root system architecture and symbiotic nodulation by a receptor-like kinase. *PLoS Genet* **10**, e1004891 (2014).
8. Endo, M., Shimizu, H. & Araki, T. Rapid and simple isolation of vascular, epidermal and mesophyll cells from plant leaf tissue. *Nat Protoc* **11**, 1388-1395 (2016).
9. Ogilvie, H.A., Imin, N. & Djordjevic, M.A. Diversification of the *C-TERMINALLY ENCODED PEPTIDE* (*CEP*) gene family in angiosperms, and evolution of plant-family specific *CEP* genes. *BMC Genomics* **15**, 870 (2014).
10. Rouhier, N., Couturier, J. & Jacquot, J.P. Genome-wide analysis of plant glutaredoxin systems. *J Exp Bot* **57**, 1685-1696 (2006).
11. Gutsche, N., Thurow, C., Zachgo, S. & Gatz, C. Plant-specific CC-type glutaredoxins: functions in developmental processes and stress responses. *Biol Chem* **396**, 495-509 (2015).
12. Xing, S., Rosso, M.G. & Zachgo, S. ROXY1, a member of the plant glutaredoxin family, is required for petal development in *Arabidopsis thaliana*. *Development* **132**, 1555-1565 (2005).
13. Xing, S. & Zachgo, S. *ROXY1* and *ROXY2*, two *Arabidopsis* glutaredoxin genes, are required for anther development. *Plant J* **53**, 790-801 (2008).
14. Patterson, K. *et al.* Nitrate-regulated glutaredoxins control *Arabidopsis* primary root growth. *Plant Physiol* **170**, 989-999 (2016).
15. Filleur, S. & Daniel-Vedele, F. Expression analysis of a high-affinity nitrate transporter isolated from *Arabidopsis thaliana* by differential display. *Planta* **207**, 461-469 (1999).
16. Chiou, T.J. & Lin, S.I. Signaling network in sensing phosphate availability in plants. *Annu Rev Plant Biol* **62**, 185-206 (2011).

17. Vert, G.A., Briat, J.F. & Curie, C. Dual regulation of the *Arabidopsis* high-affinity root iron uptake system by local and long-distance signals. *Plant Physiol* **132**, 796-804 (2003).

18. Okamoto, S., Shinohara, H., Mori, T., Matsubayashi, Y. & Kawaguchi, M. Root-derived CLE glycopeptides control nodulation by direct binding to HAR1 receptor kinase. *Nat Commun* **4**, 2191 (2013).

19. Driscoll, S.P., Prins, A., Olmos, E., Kunert, K.J. & Foyer, C.H. Specification of adaxial and abaxial stomata, epidermal structure and photosynthesis to CO_2 enrichment in maize leaves. *J Exp Bot* **57**, 381-390 (2006).

20. Kuromori, T. *et al.* A collection of 11 800 single-copy *Ds* transposon insertion lines in *Arabidopsis*. *Plant J* **37**, 897-905 (2004).

21. Alonso, J.M. *et al.* Genome-wide insertional mutagenesis of *Arabidopsis thaliana*. *Science* **301**, 653-657 (2003).

22. Turnbull, C.G., Booker, J.P. & Leyser, H.M. Micrografting techniques for testing long-distance signalling in *Arabidopsis*. *Plant J* **32**, 255-262 (2002).

Acknowledgments

We thank Yukiko Sugisawa (The University of Tokyo) for the microarray analysis. This research was supported by a Grant-in-Aid for Scientific Research (S) (number 25221105) and a Grant-in-Aid for Scientific Research on Innovative Areas (number 15H05957) from Japan Society for Promotion of Science.

Author contributions

Y.M. conceived this project and designed the experiments with input from Y.O., M.T., R.T. and M.O.-O. All authors performed the experiments and interpreted the results. Y.M. wrote the manuscript with input from Y.O.

Additional information

Supplementary information is available online. Reprints and permissions information is available online at www.nature.com/reprints. Correspondence and requests for materials should be addressed to Y.M.

Competing interests

The authors declare no competing financial interests.

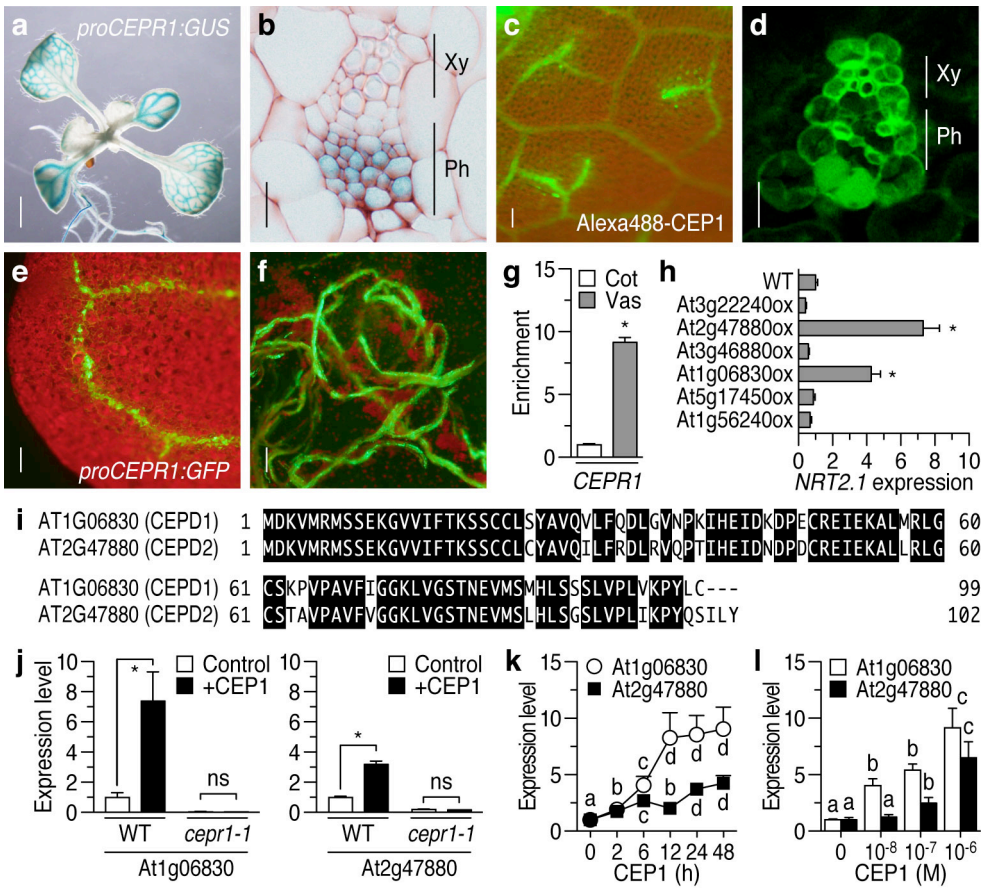

Fig. 1. Identification and characterization of At1g06830 (CEPD1) and At2g47880 (CEPD2) polypeptides. (**a**) Histochemical staining of 10-day-old seedlings transformed with the *CEPR1pro:GUS* gene. Scale bar = 1 mm. (**b**) Cross-section of the leaf vascular tissues pictured in (a). Scale bar = 10 μm. (**c**) Accumulation of the root-derived Alexa488-CEP1 signals in leaf veins. Scale bar = 100 μm. (**d**) Cross-section of the leaf vascular tissues pictured in (c). Scale bar = 10 μm. (**e**) Fluorescent micrograph of *CEPR1pro:GFP* expression in cotyledons of 7-day-old seedlings. Scale bar = 100 μm. (**f**) Mechanically isolated vascular tissues of cotyledons. GFP signals confirm the recovery of CEPR1-expressing phloem cells. Scale bar = 100 μm. (**g**) Enrichment of *CEPR1* transcripts in the collected tissues determined by quantitative reverse transcription PCR (qRT-PCR). (**h**) qRT-PCR of *NRT2.1* transcripts in the roots of transgenic plants overexpressing each gene grown on the N-rich medium (10 mM NO_3^- and 10 mM NH_4^+) (mean ± SD, *P < 0.05 by Student's *t* test, n = 3). (**i**) Sequence alignment of At1g06830 (CEPD1) and At2g47880 (CEPD2) polypeptides. Identical residues are boxed in black. (**j**) qRT-PCR of *At1g06830* and *At2g47880* transcripts in the leaves of 9-day-old wild-type (WT) and *cepr1-1* plants grown on the N-rich medium in the presence or absence of 1 μM CEP1 (n = 3). (**k**) Time course of the induction of *At1g06830* and

At2g47880 after the CEP1 treatment. Letters indicate statistically significant differences (mean ± SD, $P < 0.05$, one-way ANOVA followed by Tukey's test, n = 3). (**I**) Dose-dependence of *At1g06830* and *At2g47880* induction by CEP1 (n = 3).

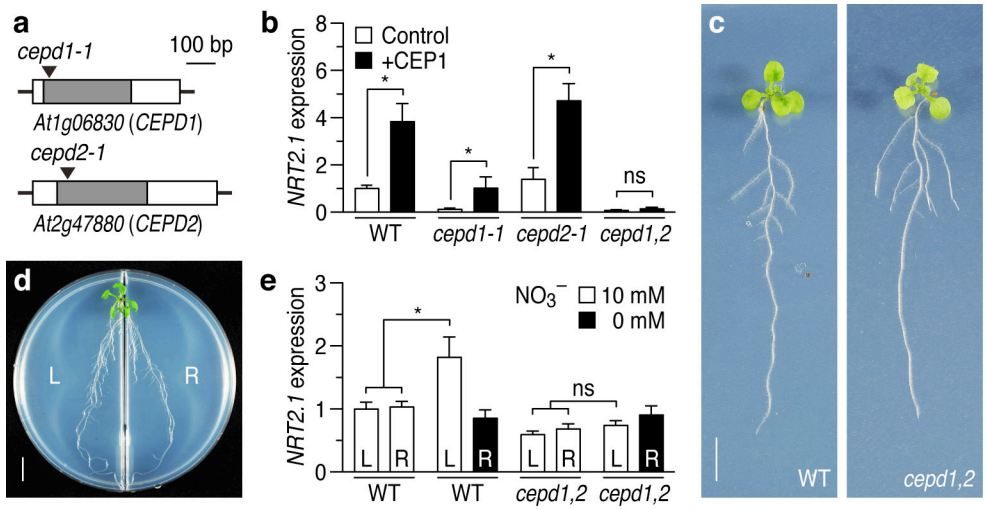

Fig. 2. CEPD1 and CEPD2 are required for systemic nitrogen acquisition. (**a**) Schematic representation of the T-DNA insertion sites in *cepd1-1* and *cepd2-1*. T-DNA was inserted 20 bp and 36 bp after the start codon of *CEPD1* and *CEPD2*, respectively. (**b**) qRT-PCR of *NRT2.1* transcripts in the roots of 9-day-old single and double mutant plants grown on the N-rich medium (10 mM NO_3^- and 10 mM NH_4^+) in the presence or absence of 1 μM CEP1. (**c**) Phenotypes of 12-day-old seedlings of the *cepd1-1 cepd2-1* double mutant. Scale bar = 5 mm. (**d**) Split-root culture system in which the root system of a plant is separated into left (L) and right (R) parts that are exposed to different nutrient conditions (10 mM NO_3^- or no N). Scale bar = 1 cm. (**e**) qRT-PCR of *NRT2.1* transcripts on each side of the split-root system of wild-type and *cepd1-1 cepd2-1* plants, in which one side of the root system was starved for N for 24 h (n = 3).

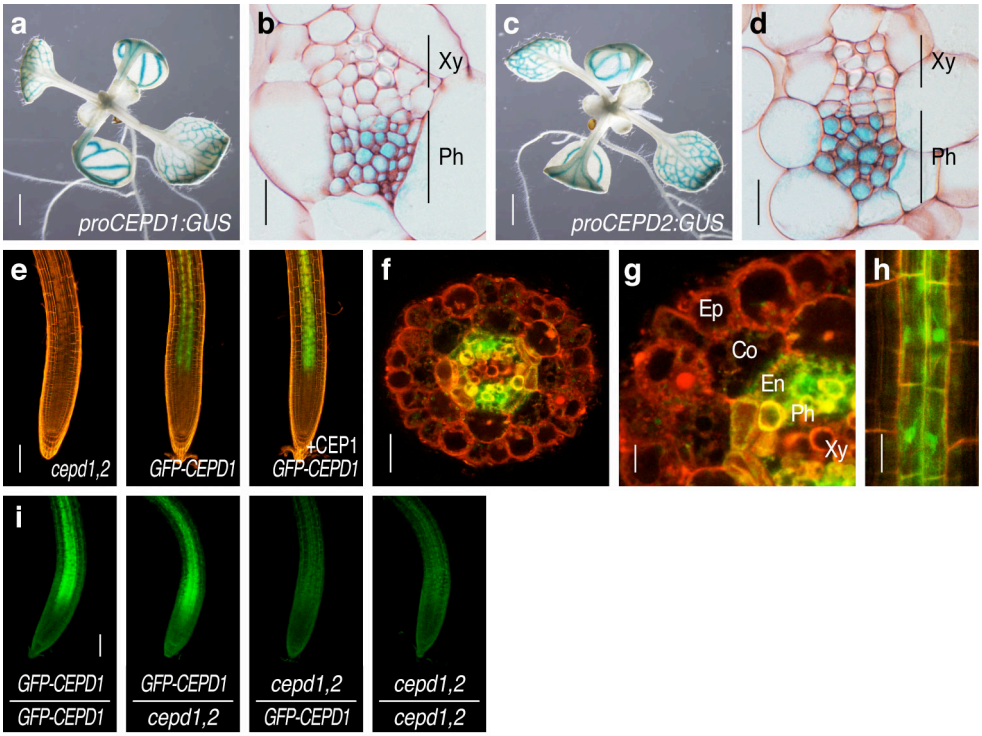

Fig. 3. CEPD1 and CEPD2 are shoot-to-root mobile signals. (**a**) Histochemical staining of 10-day-old seedlings transformed with the *CEPD1pro:GUS* gene. Scale bar = 1 mm. (**b**) Cross-section of the leaf vascular tissues pictured in (a). Scale bar = 10 μm. (**c**) Histochemical staining of *CEPD2pro:GUS* plants. Scale bar = 1 mm. (**d**) Cross-section of the leaf vascular tissues in (c). Scale bar = 10 μm. (**e**) Detection of the GFP-CEPD1 signals in the root vascular region of 9-day-old *cepd1-1 cepd2-1* plants complemented by *GFP-CEPD1*, treated with or without 1 μM CEP1 for 24 h, on the N-rich medium (10 mM NO_3^- and 10 mM NH_4^+). Scale bar = 100 μm. (**f**) Vibratome section of the roots of *GFP-CEPD1*-complemented plants grown in the presence of CEP1. Scale bar = 25 μm. (**g**) Enlarged view of (f). Abbreviations: Ep, epidermis; Co, cortex; En, endodermis; Ph, phloem; Xy, xylem. Scale bar = 10 μm. (**h**) Close view of the endodermis cell layer in (e). Scale bar = 20 μm. (**i**) Detection of the GFP-CEPD1 signals in the root vascular region of reciprocally grafted plants. Scale bar = 100 μm.

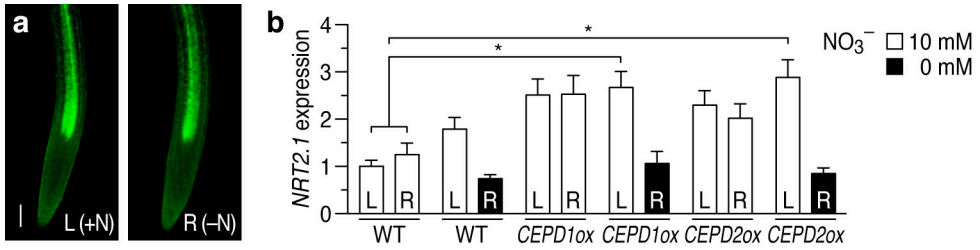

Fig. 4. Distribution and action of CEPD1 and CEPD2 under split-root conditions. (**a**) Distribution of the GFP-CEPD1 signals in each side of the split-root system in which one side of the root system was starved for N for 24 h and the other side was kept under an N-rich condition (10 mM NO_3^-). Scale bar = 100 μm. (**b**) qRT-PCR of *NRT2.1* transcripts on each side of the split-root system of *CEPD1*-overexpressing (*CEPD1ox*) plants or *CEPD2*-overexpressing (*CEPD2ox*) plants, in which one side of the root system was starved for N for 24 h (n = 3).

Supplementary Materials for

Shoot-to-root mobile polypeptides involved in systemic regulation of nitrogen acquisition

Yuri Ohkubo[1], Mina Tanaka[1], Ryo Tabata, Mari Ogawa-Ohnishi and Yoshikatsu Matsubayashi*

[1]These authors contributed equally to this work
Correspondence to: matsu@bio.nagoya-u.ac.jp

This PDF file includes:

Supplementary Fig. 1 to 7
Supplementary Table 1 and 2

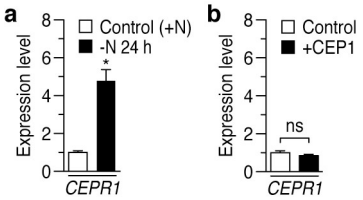

Supplementary Fig. 1. *CEPR1* expression is upregulated by N-starvation. (**a**) qRT-PCR of *CEPR1* transcripts in the shoots of 14-day wild-type plants grown on the N-rich medium (NH_4^+ 10 mM, NO_3^- 10 mM) after N-starvation of the roots for 24 h (mean ± SD, *P < 0.05 by Student's *t* test, n = 3). (**b**) qRT-PCR of *CEPR1* transcripts in the shoots after roots were treated with 1 μM CEP1 for 24 h.

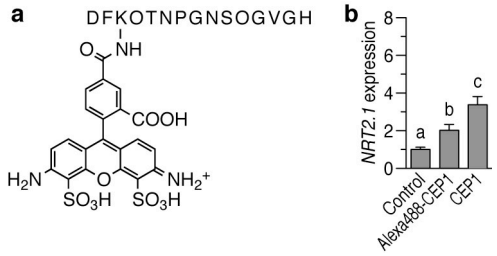

Supplementary Fig. 2. Structure and activity of Alexa488-CEP1. (**a**) Structure of Alexa488-CEP1. (**b**) qRT-PCR of *NRT2.1* transcripts in the roots of wild-type plants grown on the N-rich medium after peptide treatment at 1 μM for 9 days. Letters indicate statistically significant differences (mean ± SD, P < 0.05, one-way ANOVA followed by Tukey's test, n = 3).

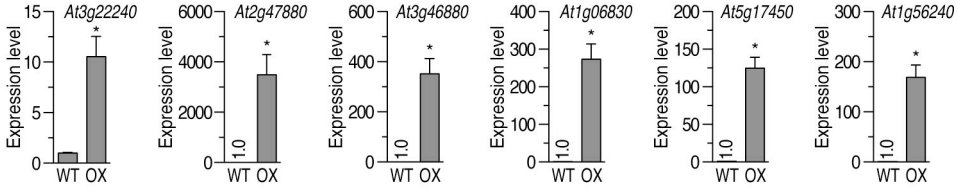

Supplementary Fig. 3. Overexpression of 6 primary candidate genes. qRT-PCR of transcripts of each transgene in 9-day seedlings of transgenic plants grown on the N-rich medium (n = 3).

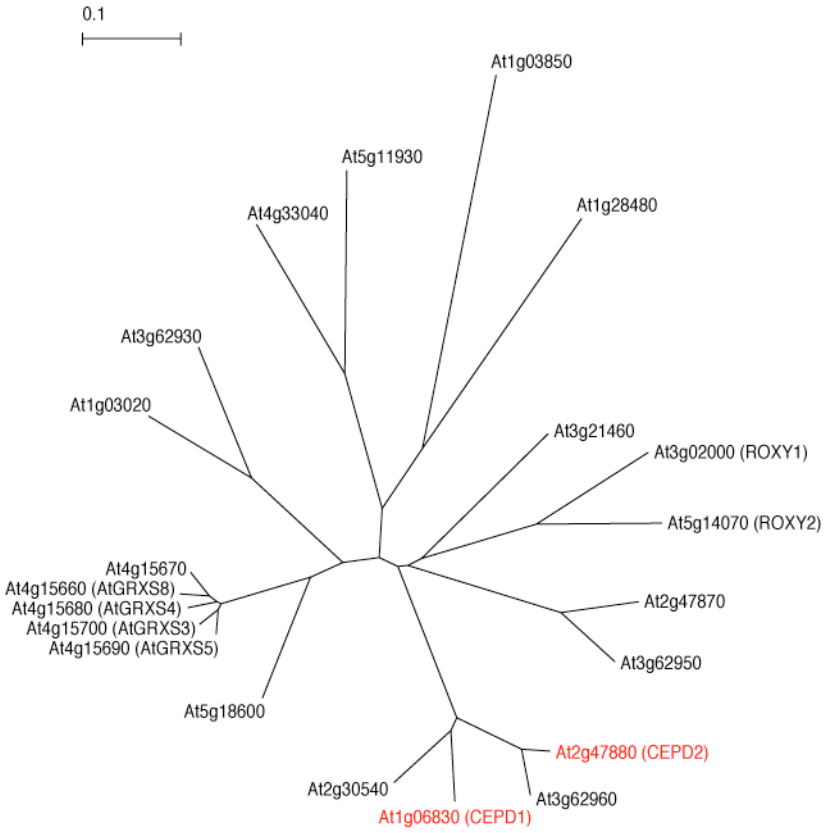

Supplementary Fig. 4. Phylogenetic tree of the class III glutaredoxin family. The class III glutaredoxin family comprises 21 members in *Arabidopsis*.

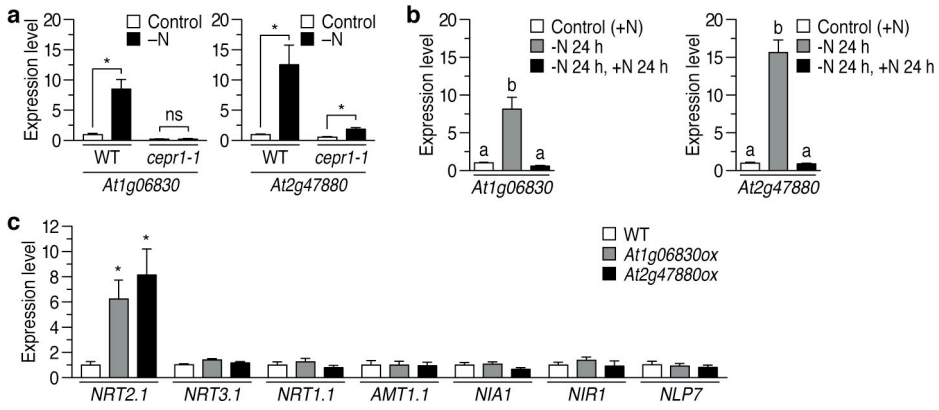

Supplementary Fig. 5. Functional analysis of At1g06830 and At2g47880. (**a**) qRT-PCR of At1g06830 and At2g47880 transcripts in the leaves of 14-day-old wild-type and *cepr1-1* plants after N-starvation for 24 h (n = 3). (**b**) qRT-PCR of At1g06830 and At2g47880 transcripts in the leaves of wild-type plants subjected to N-starvation for 24 h, followed by N-resupply (NH_4^+ 10 mM, NO_3^- 10 mM) for 24 h (n = 3). (**c**) Overexpression of At1g06830 and At2g47880 specifically induced *NRT2.1* but not *NRT3.1*, *NRT1.1*, and other N-regulated genes (n = 3).

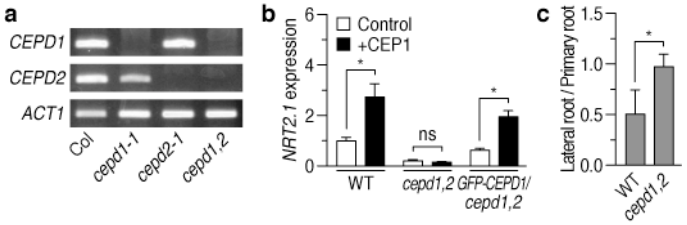

Supplementary Fig. 6. Characterization of *cepd1-1* and *cepd2-1* mutants. (**a**) Absence of full-length transcripts in *cepd1-1* and *cepd2-1* mutants revealed by RT-PCR. (**b**) Complementation of the *cepd1-1 cepd2-1* double mutant phenotype with *GFP-CEPD1* expressed under the control of its native promoter (n = 3). (**c**) Lateral root length of 12-day-old wild-type and *cepd1-1 cepd2-1* mutant seedlings (n = 5).

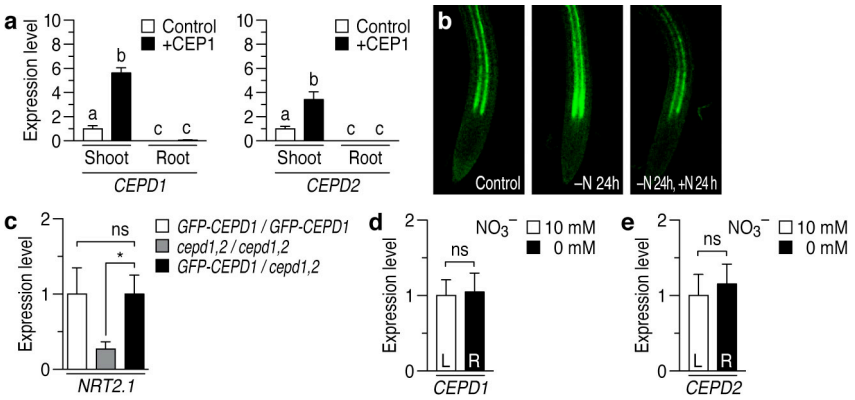

Supplementary Fig. 7. Expression of *CEPD1* and *CEPD2*. (**a**) qRT-PCR of *CEPD1* and *CEPD2* transcripts in the shoots and the roots of 9-day-old wild-type plants cultured on the N-rich medium in the presence or absence of CEP1 (n = 3). (**b**) Detection of the GFP-CEPD1 signals in the root vascular region of 10-day-old *GFP-CEPD1*-complemented plants subjected to N-starvation for 24 h, followed by N-resupply for 24 h. (**c**) qRT-PCR of *NRT2.1* transcripts in the roots of reciprocally grafted plants 12 days after grafting (n = 3). (**d**) qRT-PCR of *CEPD1* transcripts on each side of the split-root system of *CEPD1ox* plants, in which one side of the root system was starved for N for 24 h (n = 3). (**e**) qRT-PCR of *CEPD2* transcripts on each side of the split-root system of *CEPD2ox* plants (n = 3).

Supplementary Table 1. A list of the CEP1-regulated genes in vascular tissues. Total RNA was isolated from the vascular tissues of cotyledons of 8-day-old wild type, wild type grown on the N-rich medium containing 1 μM CEP1, and *cepr1-1* mutant seedlings. The table includes the GeneChip signal intensity, signal intensity ratio, Z-score, gene description, presence of orthologs in other species, presence of N-terminal secretion signal sequence, and predicted protein size. Six conserved genes encoding small proteins with no predicted secretion signal are marked in red.

Signal intensity			Ratio		Z-score		Gene				Protein	
WT	+CEP	*cepr1-1*	+CEP/W	*cepr1*/W	+CEP/W	*cepr1*/W	Locus	Symbol	Description	Orthologs	Signal P	Length (aa)
31.6	211.6	4.2	6.69	0.13	20.98	-3.52	At5g46871	---	Encodes a defensin-like (DEFL) family	N	Y	78
18.9	116.1	8.9	6.13	0.47	18.91	-2.17	At3g22240	---	---	Y	N	72
26.5	108.2	9.3	4.08	0.35	11.34	-2.65	At2g15480	UGT73B5	UDP-glucosyl transferase 73B5	Y	N	484
16.3	57.0	8.2	3.50	0.50	9.19	-2.05	At3g47090	---	LRR protein kinase family	Y	Y	1009
456.6	1577.4	82.6	3.45	0.18	9.01	-3.32	At3g49780	PSK4	Phytosulfokine 4 precursor	Y	Y	79
16.6	55.3	3.4	3.32	0.21	8.53	-3.20	At2g47880	---	Glutaredoxin family protein	Y	N	102
99.7	321.3	41.2	3.22	0.41	8.16	-2.41	At3g28007	SWEET4	Nodulin MtN3 family protein	Y	Y	251
80.5	252.2	11.2	3.14	0.14	7.86	-3.48	At3g46880	---	---	Y	N	153
175.9	512.3	10.5	2.91	0.06	7.01	-3.80	At1g06830	---	Glutaredoxin family protein	Y	N	99
22.0	58.5	10.6	2.67	0.48	6.13	-2.13	At4g28490	HAESA	LRR receptor-like protein kinase	Y	Y	999
55.3	141.6	17.7	2.56	0.32	5.72	-2.77	At1g44800	SIAR1	Nodulin MtN21 family	Y	Y	370
283.6	701.0	72.1	2.47	0.25	5.39	-3.04	At1g67860	---	---	N	Y	78
477.6	1090.2	177.5	2.28	0.37	4.68	-2.57	At5g17450	HIPP21	Heavy metal transport/detoxification family	Y	N	149
9.1	19.3	4.2	2.12	0.46	4.09	-2.21	At1g56240	PP2-B13	Phloem protein 2-B13	Y	N	284
13.3	28.0	6.1	2.12	0.46	4.09	-2.21	At2g05632	---	---	N	N	52
77.2	163.3	11.6	2.11	0.15	4.06	-3.44	At3g24230	---	Pectate lyase family protein	Y	Y	452
24.6	51.5	6.9	2.09	0.28	3.98	-2.92	At3g14385	MIR169F	miRNA	Y	–	–

Supplementary Table 2. Microarray expression data of the 4 genes in the At1g06830/At2g47880 subfamily. The table includes the GeneChip signal intensity, signal intensity ratio, Z-score, and gene description of these 4 genes.

Signal intensity			Ratio		Z-score		Gene				Protein	
WT	+CEP	*cepr1-1*	+CEP/W	*cepr1*/W	+CEP/W	*cepr1*/W	Locus	Symbol	Description	Orthologs	Signal P	Length (aa)
16.6	55.3	3.4	3.32	0.21	8.53	-3.20	At2g47880	---	Glutaredoxin family protein	Y	N	102
175.9	512.3	10.5	2.91	0.06	7.01	-3.80	At1g06830	---	Glutaredoxin family protein	Y	N	99
4.3	4.3	4.3	1.00	0.98	-0.05	-0.13	At3g62960	---	Glutaredoxin family protein	Y	N	102
141.7	124.2	104.3	0.88	0.74	-0.49	-1.09	At2g30540	---	Glutaredoxin family protein	Y	N	102